Chapter I

Magneto-optical study of Cr-doped CdTe quantum dots

The main goal of this thesis was to include single Cr atoms in CdTe/ZnTe QDs. It was successfully achieved. We saw in the Sec. **??** that the magnetic anisotropy of the Cr spin induced by local strains leads to a zero magnetic field splitting of the $S_z = 0$, ± 1 and ± 2 states. In this chapter, we optically probe Cr-doped QDs in order to study the carrier-Cr interactions.

We begin presenting the photoluminescence (PL) and the energy structure of the X-Cr complex. It was sawn that the exchange interaction between the carrier and the Chromium is strong enough to see the effect of a single Cr spin in the quantum dots, giving the PL of the dots four characteristics peaks. We discuss the evolution of the emission in temperature and present different excited states of the system. Magneto-optical experiments confirm the energy structure, and hints at an anti-ferromagnetic between hole and Cr. In the next section, we use the evolution of the QDs PL under magnetic field in order to construct a spin hamiltonian model including the strain induced fine structure of the magnetic atom, the exchange coupling with the carriers and the influence of the reduced symmetry of the QDs on the electron-hole exchange interaction and on the valence band. In the last section, we present dots having the characteristic four peaks PL, but that are not explained by our model. We finish proposing a possible explanation for those dots.

I.1 Strained quantum dots containing an individual X-Cr atom

I.1.1 Energy structure of X-Cr in a quantum dot

Using the procedure described in the Sec. II.1, we randomly incorporated Cr atoms in CdTe/ZnTe quantum dots, adjusting the density of the Cr atoms to be roughly equal to the density of dots, in order to get QDs containing 0, 1 or a few Cr atoms. The photoluminescence (PL) of individual QDs, induced by optical excitation with a dye laser tuned on resonance with an excited state of the dots, is studied by optical micro-spectroscopy.

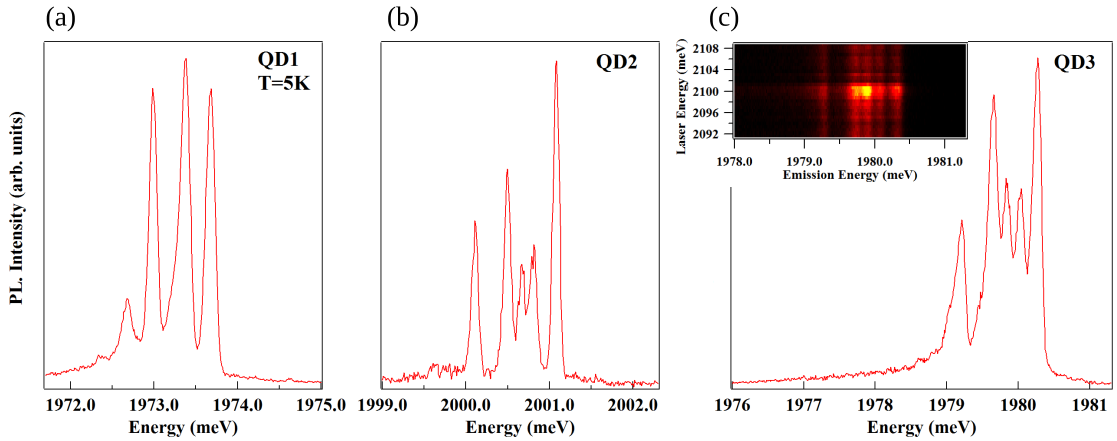

Figure I.1: PL of (a) QD1, (b) QD2 and (c) QD3 X-Cr complex at low temperature (T=5K). Inset in (c) presents the PLE map of this QD, showing a sharp quasi-resonant state for an excitation at 2100 meV.

Low temperature (T=5K) PL of the neutral exciton (X-Cr) of several QDs doped with a single Cr are reported in Fig. I.1. A characteristic three emission lines is observed, with a fourth, weaker peak on the low energy side. In some QDs, such as QD2 and QD3, the central peak was found to be split. Scanning with an energy tunable laser, we saw that all the peaks share a common quasi-resonant state, where all are at a maximum intensity, as highlighted in the inset of Fig. I.1(c). This is an indication that they originate from the same dot. Variations in the relative intensities of the peaks are observed in different dots.

In a II-VI semiconductor, the orbital momentum of the Cr connects the spin of the atom to its local strain environment through the modification of the crystal field and the spin-orbit coupling. For biaxial strain in the (001) plane, the ground state of a Cr spin is split by a strain induced magnetic anisotropy term $\mathcal{H}_{Cr,\varepsilon_\parallel} =$

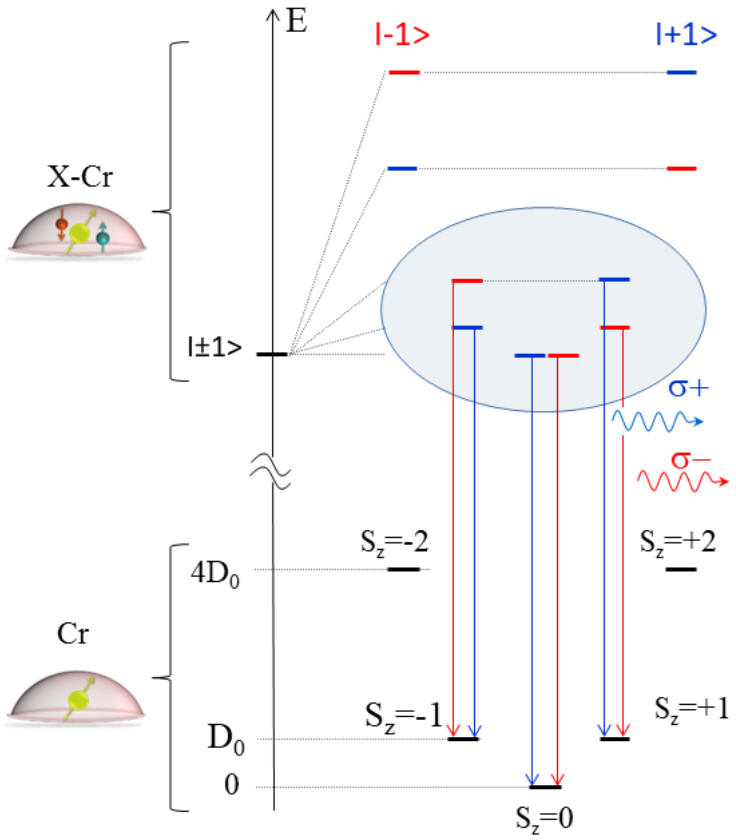

Figure I.2: Illustration of the energy levels of the ground state (Cr), the bright exciton states ($|\pm 1\rangle$) coupled to the spin of a Cr (X-Cr) and dominant PL transitions ($\sigma+$, σ-). The states $S_z = \pm 2$ cannot be populated through thermalization, and thus their recombination channel are not shown on this schema.

$D_0 S_z^2$ (see Sec. **??**). It was deduced from electron paramagnetic resonance of bulk Cr-doped CdTe that D_0 is positive for compressive biaxial strain [1]. In a self-assembled CdTe/ZnTe QDs with large in-plane strain, the Cr spin energy levels are split from $|S_z = 0\rangle$ at low energy (Fig. I.2). A value of D_0 in the 1 meV range can be expected for a CdTe layer strained on a ZnTe substrate, as shown in Sec. **??**.

When an electron-hole pair is injected in a Cr-doped QD, the bright excitons are split by the exchange interaction between the spins of Cr and carriers. In flat self-assembled QDs, the heavy-holes and light-holes are separated in energy by the biaxial strain and the confinement. In a first approximation, the ground state in such QD is a pure heavy-hole (J_z=$\pm 3/2$) exciton and the exchange interaction

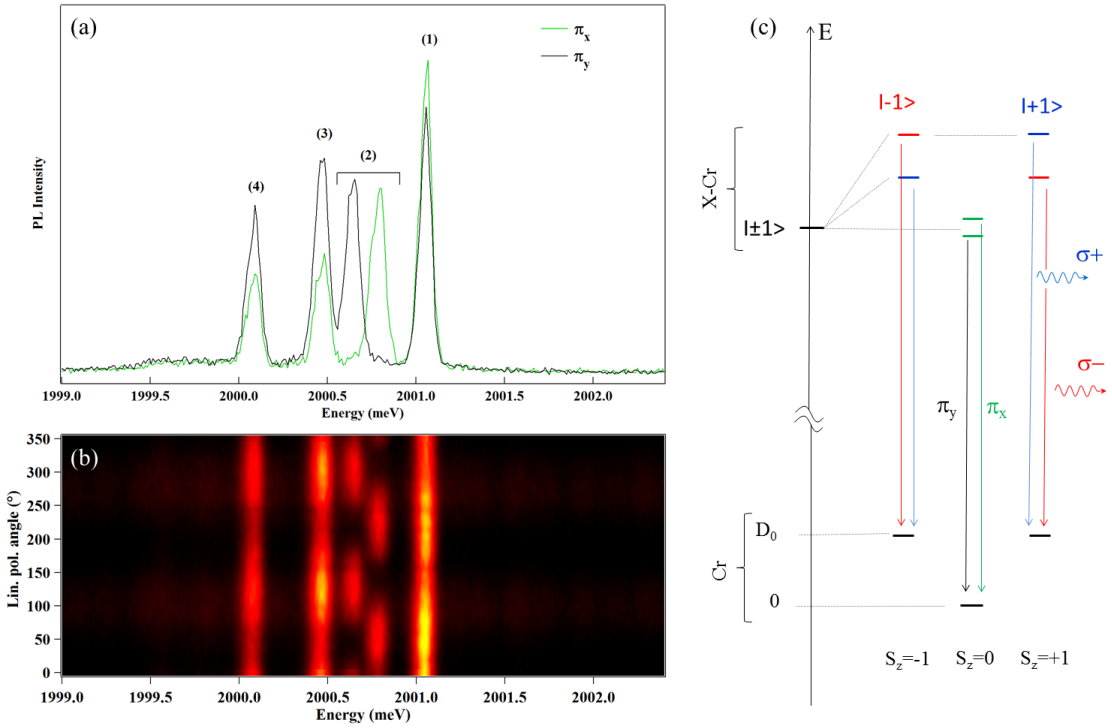

Figure I.3: (a) Low temperature PL of QD2 recorded along two orthogonal directions. (b) Linear polarization PL intensity map of QD2. The 0° polarization angle corresponds to an emission polarized along the QD cleavage axis, either [110] or [1$\bar{1}$0]. (c) Illustration of the energy levels of the ground state (Cr), the bright exciton states ($|\pm 1\rangle$) coupled to the spin of a Cr (X-Cr), showing the splitting of the central peak via the bright exciton coupling, and dominant PL transitions ($\sigma+$ (blue), $\sigma-$ (red) and π (green and black)).

with the Cr spin S is described by the spin Hamiltonian

$$\mathcal{H}_{c-Cr} = I_{eCr}\mathbf{S}\cdot\boldsymbol{\sigma} + I_{hCr}S_zJ_z \tag{I.1}$$

with $\boldsymbol{\sigma}$ the electron spin and J_z the hole spin operator. I_{eCr} and I_{hCr} are, respectively, the exchange integrals of the electron and the hole spins with the Cr spin. These exchange energies depend on the exchange constant of the Cr $3d$ electrons with the CdTe carriers and on the overlap of the Cr atom with the confined carriers. Even though the exchange interaction of the Cr spin with both electron and hole is ferromagnetic in most II-VI semiconductor [2–4], the hole-Cr interaction is supposed to be anti-ferromagnetic here. It does not change the PL at B = 0T. The only visible effect is on the intensity distribution in the magneto-optics experiments. This will thus be further discussed in Sec. I.1.3. A typical exchange

constant 4 to 5 times larger for the holes than for the electrons is also expected in CdTe [5, 6].

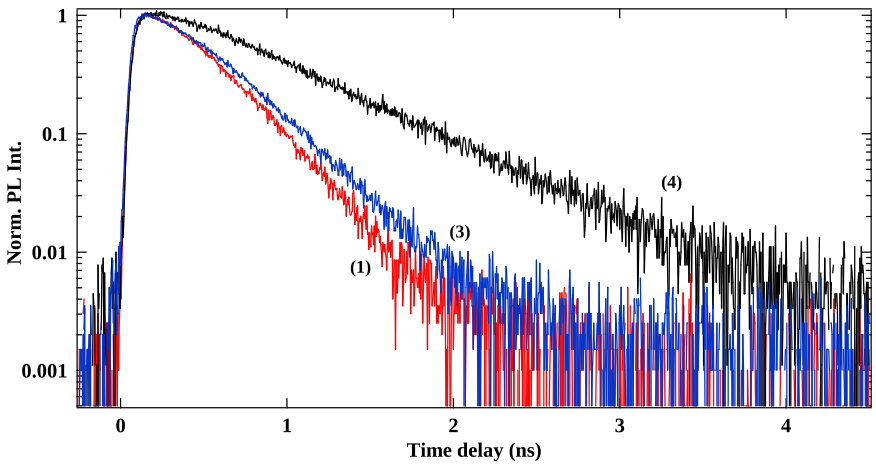

Figure I.4: Time resolved PL of QD2 taken on two outside peaks, attributed to $S_z = \pm 1$ (noted (1) and (3) in Fig. I.3(a)), and the lower energy one (noted (4)).

For highly strained CdTe/ZnTe QDs with a weak hole confinement, the strain induced energy splitting of the Cr spin $D_0 S_z^2$ is much larger than the exchange energy with the confined carriers ($D_0 \gg |I_{hCr}| > |I_{eCr}|$). The exchange interaction with the exciton acts as an effective magnetic field which further splits the Cr spins states $S_z = \pm 1$ and $S_z = \pm 2$. The resulting X-Cr energy levels are presented in Fig. I.2. The exciton recombination does not affect the Cr atom and its spin is conserved during the optical transitions. Consequently, the large strain induced splitting of the Cr spin is not directly observed in the optical spectra. However, at low temperature, the Cr spin thermalize on the low energy states S_z=0 and S_z=$\pm$1. This leads to a PL dominated by three contributions: a central line corresponding to $S_z = 0$ and the two outer lines associated with $S_z = \pm 1$ split by the exchange interaction with the carriers.

Cr-doped quantum dots exhibit a linear polarization dependence, as presented in Fig. I.3. The central line (S_z=0) is split and linearly polarized along two orthogonal directions. As in non-magnetic QDs, this results from a coupling of the two bright excitons $|\pm 1\rangle$ by (i) the long-range e-h exchange interaction in a QD with an in-plane shape anisotropy [7] and/or (ii) the short range e-h exchange interaction in the presence of valence band mixing. This anisotropic e-h exchange energy mixes the bright exciton associated with the same Cr spin state, inducing an extra splitting between them. The mixing is maximum for the central pair of bright excitons (S_z=0) which are initially degenerated. The outer lines are also slightly

linearly polarized but the influence of the e-h exchange interaction is attenuated by the initial splitting of the $|\pm 1\rangle$ excitons induced by the exchange interaction with the Cr spin$S_z = \pm 1$.

In order to identify the lower energy peak ((4) in Fig. I.3(a)), we took the time resolved photoluminescence of the emission peaks, presented in Fig. I.4. One can notice that the line (4) present a decay time about twice as long as the high energy peak. Such a long decay would be coherent with the radiative recombination of a dark exciton state. Under normal circumstances, the recombination of such a state is non-radiative. However, it is possible to observe a dark exciton recombination emitting a photon in low symmetry quantum dot [8]. Since it is initially a forbidden transition, the recombination will be less efficient and will thus take more time [9]. This hypothesis will be confirmed by the magneto-optical study of the dot presented in Fig. I.8 and I.12.

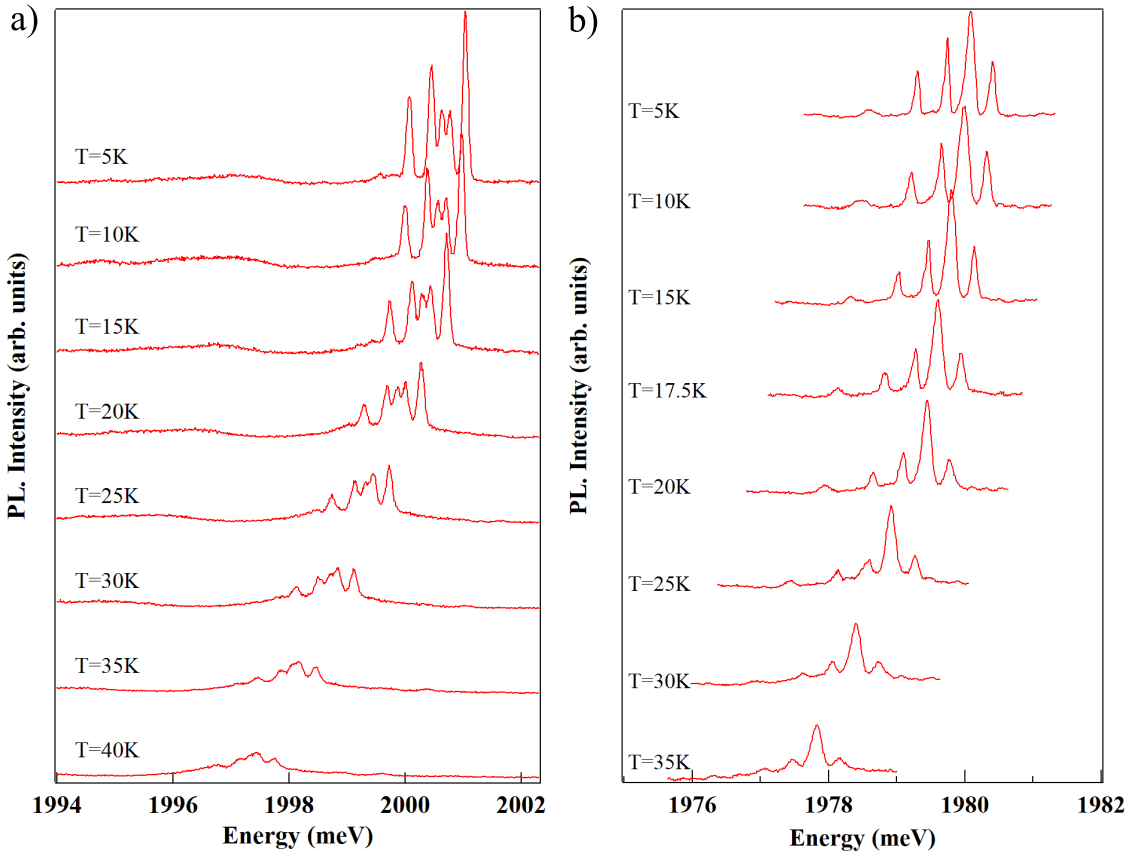

Figure I.5: Temperature evolution from T=5K to T=40K of (a) QD2 PL and (b) the PL of a QD with a good thermalisation on the low energy states (QD4). Even at 40K, $S_z = \pm 2$ states do not appear.

Since $S_z = \pm 2$ states do not appear on the PL because they cannot be thermally populated, one could expect to see their emission at higher temperature. Fig. I.5 presents the emission of two dots in function of the temperature. With the increase of the temperature, we observe a significant line broadening induced by the interaction with acoustic phonons. In order to keep a significant PL intensity and resolved PL lines, we limited our investigation to temperature below 50K. Even at this temperature, the ± 2 peak does not appear. Still, the figure of the emission change dramatically with the temperature. The intensity of the exterior peaks, associated with the states ± 1, fell quickly while the emission of the $S_z = 0$ stays intense until higher temperature. This is an unexpected picture, since the temperature should allow the higher energy states ± 1 to be more populated by emptying the ground state. This could be caused by a coupling to dark states, more efficient for $S_z = \pm 1$ states than for $S_z = 0$ states, emptying the bright states when they are thermally populated.

I.1.2 Excited states of a Cr-doped QD

In order to study the different excited states in a QD doped with a single Cr atom, we took the PLE of QD2 starting close to the energy of the dot's emission. Fig. I.6(a) presents the entire PLE of QD2 X-Cr complex. One can note several excited states along the scan.

The first remarkable feature of this scan is the luminescence over a large energy range, for an excitation between the dot emission energy and 2004 meV, zoomed in Fig. I.6 (c). This corresponds to an excitation of the QD via the acoustic phonon band. One can notice two sharp intensity diminutions in this emission. Mapping the intensity of the phonon replica to the quantum dot spectrum (Fig. I.6(d)), it shows that these diminutions happens when the laser is in resonance with a QD emission line. The absorption then preferentially occurs in this resonantly excited state than in the acoustic phonon band.

Another excited state appear around 2018.5 meV, zoomed in on Fig. I.6(f). The first feature of this peak is that, even though the studied dot contain a Cr, each of the peak here presents a slightly different resonant energy. Moreover, one can note that the order of appearance of the two central peaks seems to be reversed compared to the external ones. This phenomenon, called splitting inversion, was first observed on QDs in GaAs quantum well [10]. It has been discussed by Takagahara [7] and is likely due to the electron-hole exchange interaction.

Another excited state can be sawn at 2025 meV. It can be linked to an excitation through optical phonon. Looking at the σ polarized emissions of this state (Fig. I.7(b) and (c)), we can see that the low and high energy peaks are strongly σ_{co} polarized. It means the exciton recombining is of the same spin as the one injected by the laser, and thus shows a good spin conservation of the exciton in

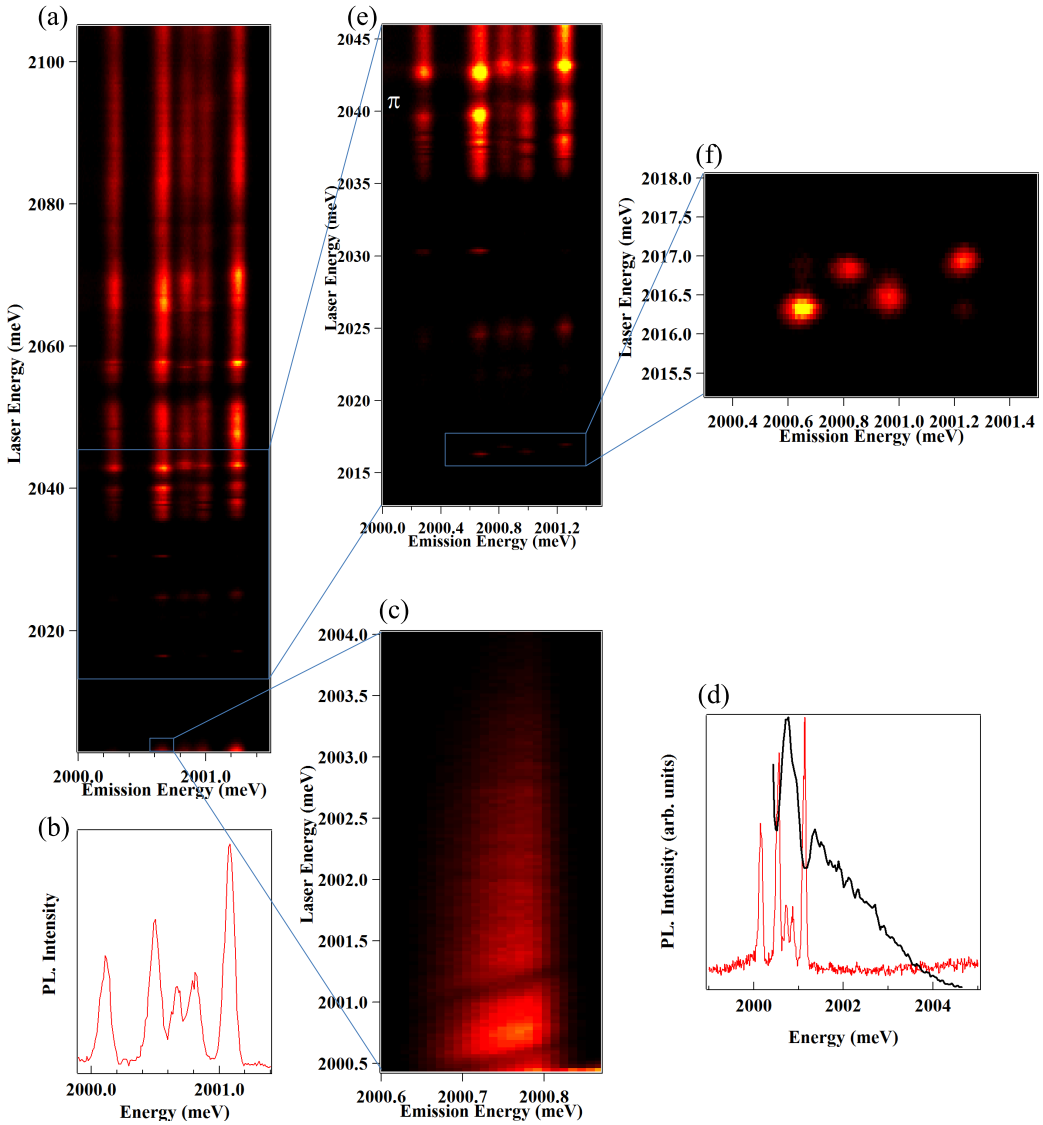

Figure I.6: (a) QD2 X-Cr PLE map in π_{cross} polarization. Several excited states are highlighted. (b) Photoluminescence of QD2 X-Cr complex for an excitation at 2120 meV). (c) PLE scan detected on the lower energy peak, taken close to the QD emission energy, showing the phonon replica taken in π detection. The emission integrated intensity in function of the laser energy is plotted in (d) (black curve) along with the PL spectra of QD2 taken in σ_{co} polarization. (e) PLE map between 2046 meV and 2013 meV presenting several excited, detecting in π_{cross} polarization. (f) Zoom in a particular excited state presented a splitting inversion, taken in π_{cross} detection.

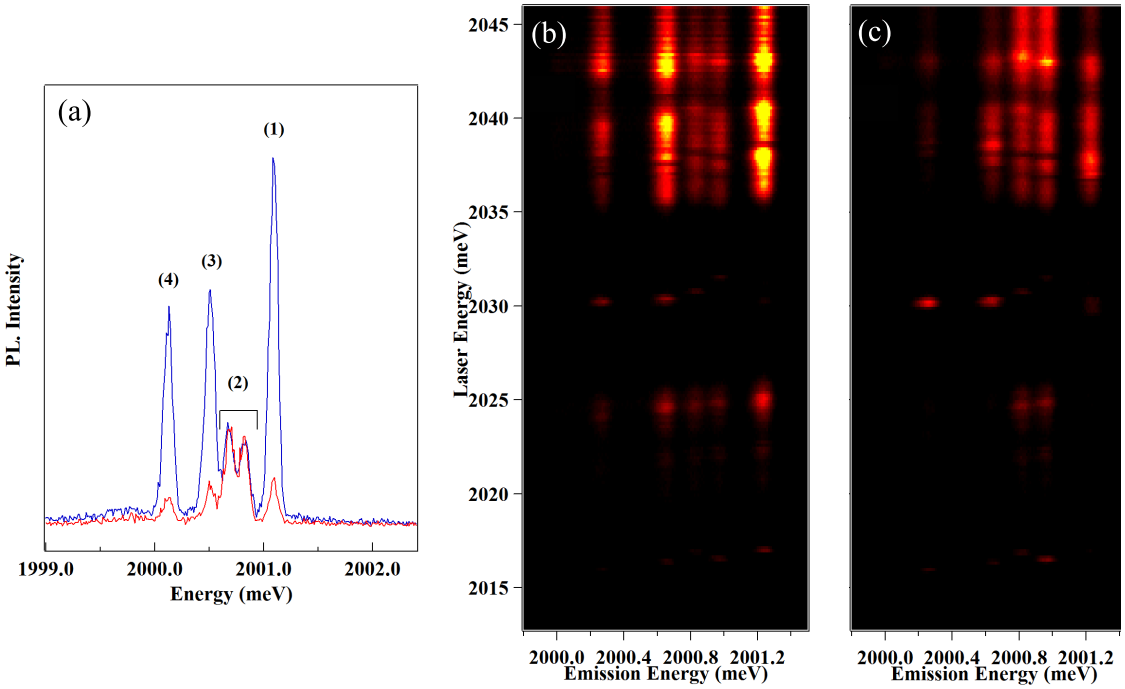

Figure I.7: (a) PL spectra of the exciton in QD2 (X-Cr) for co-circularly (blue) and cross-circularly (red) polarized excitation/detection taken on the 2120 meV quasi-resonant state. (b) - (c) PLE map between 2046 meV and 2013 meV presenting several excited states, detecting in σ_{co} (b) and σ_{cross} (c).

the QD during its lifetime. This stabilization of the exciton spin might be due to the Cr spin acting as an effective magnetic field on it. The split central peak emission is linearly polarized, as discussed in Sec. I.1.1, and thus its emission shows no dependency in linear polarization.

Finally, another interesting excited state appear at 2030 meV. This state presents an exchange-induced splitting different from the splitting in the quasi-resonant state, due to a difference in the carriers and Cr atom wavefunction overlap.

I.1.3 Magneto-optics of a quantum dot doped with a single Cr

The structure of the energy levels in Cr-doped QDs is confirmed by the evolution of the PL spectra in magnetic field (up to 11T) along the growth axis, the so called Faraday configuration [11], presented in Fig. I.8. Under magnetic field, the bright exciton $X_z = \pm 1$ split, leading to a $\sigma-$ branch going at low energy and

a $\sigma+$ one going at high energy. This splitting of the excitonunder magnetic field can compensate the one induced by the exchange interaction with the Cr [12]. For QD1, this results in an anti-crossing of $|+1\rangle$ and $|-1\rangle$ excitons due to the e-h exchange interaction around B_z=6 T observed both in $\sigma+$ and $\sigma-$ polarizations (anti-crossing (2) and (3) in Fig. I.8(a)).

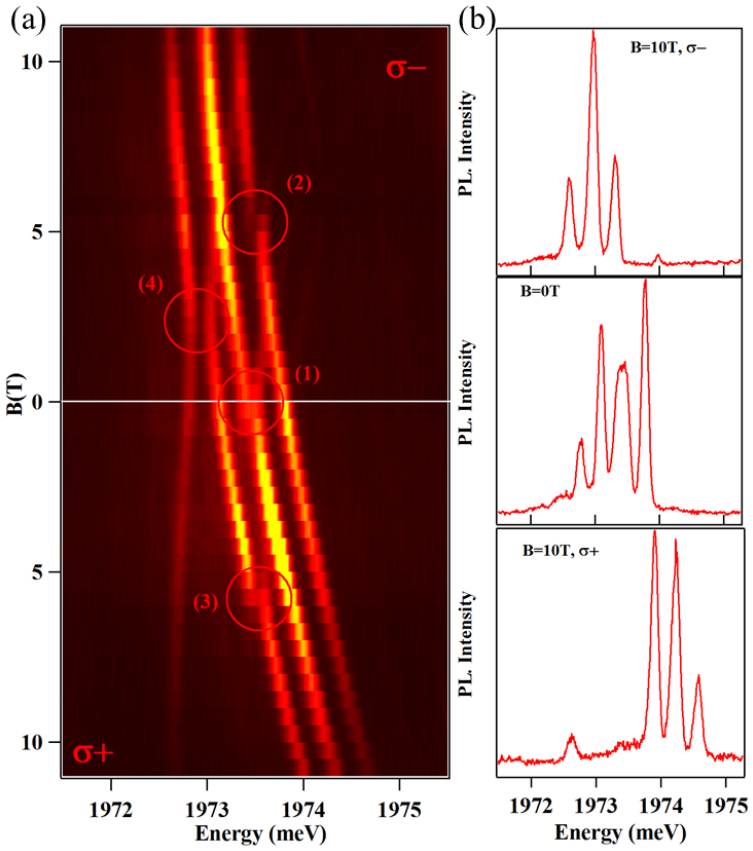

Figure I.8: (a) Circularly polarized X-Cr PL evolution under magnetic field (B_z) in QD1. Anti-crossings are highlighted and numbered. (b) QD1 X-Cr PL spectra taken at 0 and 10T for both circular polarization.

The low energy emission presented as a dark exciton in Fig. I.4 shows an anti-crossing with the bright excitons under B_z in $\sigma-$ polarization (anti-crossing (4) in Fig. I.8). This anti-crossing arises from a mixing of the bright and dark excitons interacting with the same Cr spin state. Observed in $\sigma-$ polarization, it corresponds to the mixing of the exciton states $|-1\rangle$ and $|+2\rangle$ coupled to the Cr spin $S_z = +1$. This dark/bright excitons coupling δ_{12} is induced by the e-h exchange interaction in a confining potential of reduced symmetry (lower than

C_{2v}) [13]. In such symmetry, the dark exciton acquire an in-plane dipole moment which leads to possible optical recombination at zero magnetic field [8] as observed in these QDs. The oscillator strength of this "dark exciton" increases as the initial splitting between $|-1\rangle$ and $|+2\rangle$ excitons is reduced by the magnetic field.

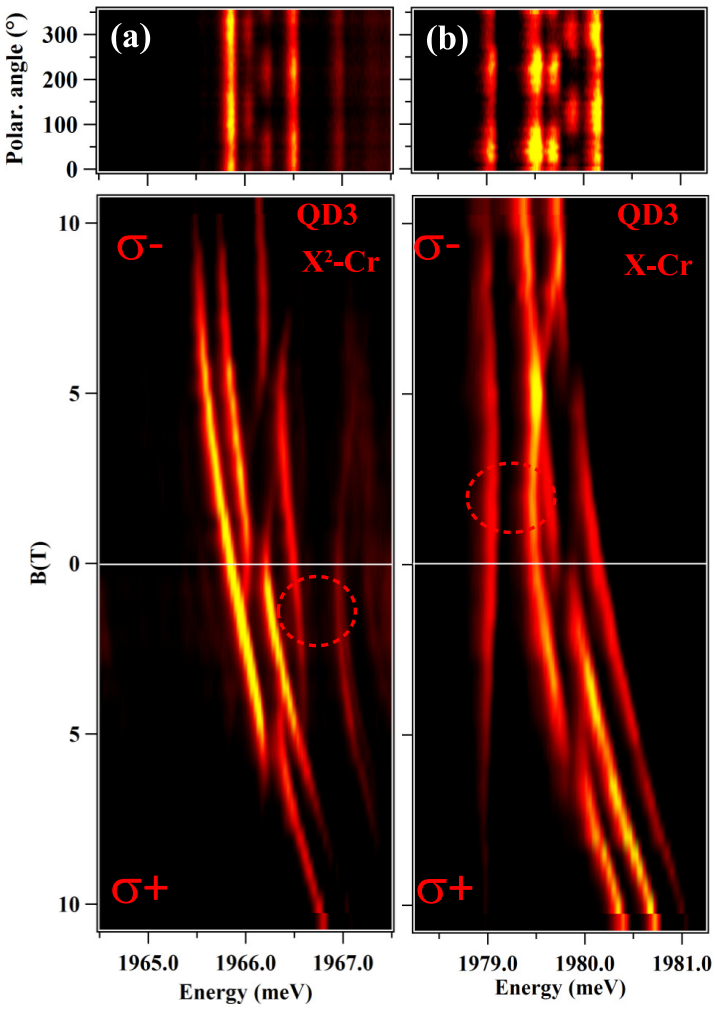

Figure I.9: Linear polarization intensity map (top panel) and intensity map of the longitudinal magnetic field dependence of the emission (bottom panel) of (a) X^2-Cr and (b) X-Cr in QD3.

To illustrate the influence of the QD symmetry on the magneto-optical properties of X-Cr, we show in Fig. I.9(b) the emission of a QD with a different strain or shape anisotropy (QD3). For QD1, the splitting of the central peak is not clear

in the PL at 0T (Fig. I.1(a)), while two linearly polarized peaks appears clearly in QD3 spectra (Fig. I.1(c)).

Investigating both the biexciton and the exciton in the same Cr-doped QD, we can also analyze the impact of the carrier-Cr interaction on the fine structure of the Cr spin. The magnetic field dependency of X^2-Cr emission in QD3 is presented along with the X-Cr emission as a contour plot in Fig. I.9(a) and (b) respectively. The PL under magnetic field of X-Cr and X^2-Cr presents a mirror symmetry. In particular, the dark/bright exciton mixing observed around $B_z = 2.5$ T on the low energy side of the PL in $\sigma-$ polarization for X-Cr is observed on the high energy side in $\sigma+$ polarization for X^2-Cr (circles in Fig. I.9(a) and (b)).

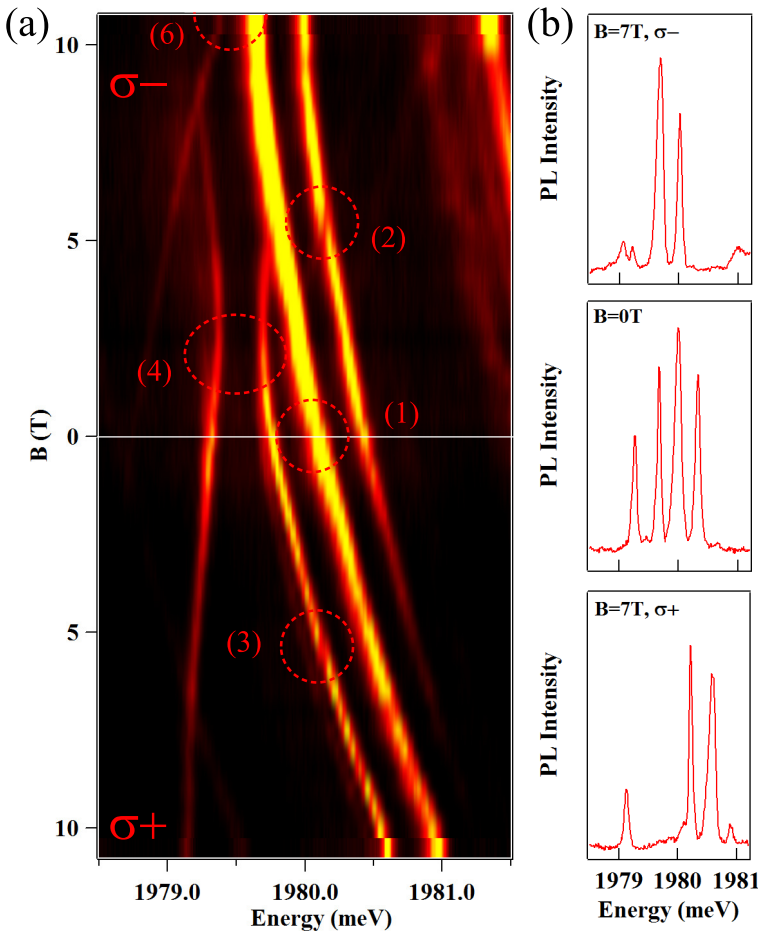

Figure I.10: (a) Evolution in magnetic field of QD4 X-Cr circularly polarized PL. (b) QD3 X-Cr PL at $B_z = 0$ T and $B_z = 7$ T in both polarization.

If one consider the ground state of X^2 as a spin-singlet (total spin 0), it cannot be split by the magnetic field or the spin interaction part of the carriers-Cr hamil-

tonian. The creation of two excitons in the QD cancels the exchange interaction with the Cr atom. Thus, the PL of X^2-Cr is controlled by the final state of the optical transitions, i.e. the eigenstates of X-Cr, resulting in the observed mirror symmetry in the PL spectra.

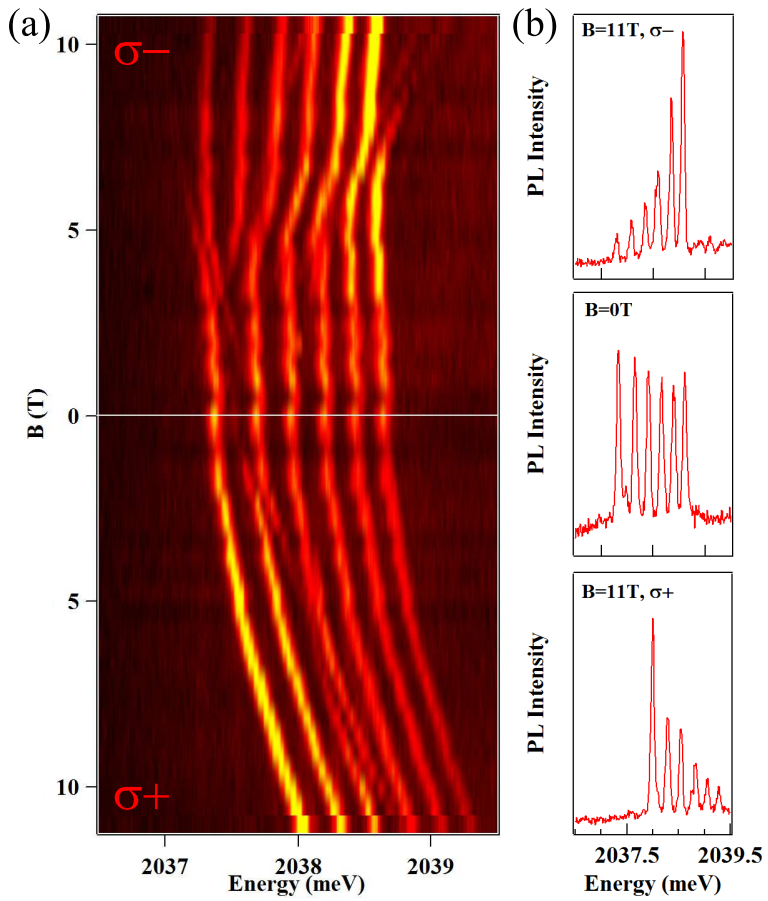

Figure I.11: (a) Evolution in magnetic field of the PL of a single Manganese atom coupled to an exciton in a II-VI QD. (b) PL spectra of the X-Mn system taken at $B_z = 0$ T and $B_z = 11$ T in both circular polarization. These experimental results are taken from Yoan Léger PhD thesis [16].

The evolution under magnetic field of the relative intensity of each of the QD peak gives information on the sign of the interaction between the Cr and the hole spin. As shown in Fig. I.2, given a polarization, each peak can be linked to a Cr spin state. As discussed earlier, applying a magnetic field lifts the degeneracy between the exciton states and allows to efficiently select the polarization of the emission. The evolution of the peaks relative intensities under magnetic thus gives

information on the hole-Cr exchange interaction sign.

QD4, presented in Fig. I.10, presents a clear evolution of the intensity under magnetic field and will be used for this study. The central peak intensity stays the stronger of the three peaks, whatever the direction of the magnetic field. This is expected, since the $S_z = 0$ state is not affected by the Zeeman effect. It remains the lower spin state for the Cr atom, and therefore concentrate most of the population. In the $\sigma-$ branch, the high energy peak get brighter while the low energy one disappear for $B_z \geq 8$T in QD4. The situation is opposite in the $\sigma+$ branch, where the intensity concentrate on the lower energy peak.

This evolution is similar as the one observed in II-VI QDs doped by a single Mn atom, presented in Fig. I.11. It was shown in Yoan Léger PhD thesis [16] that the $S_z = -\frac{5}{2}$ state of the Mn atom was stabilized under magnetic field. From the evolution of the peaks relative intensity and the polarization of the different Mn states, it was then possible to deduce that the interaction between Mn and hole was anti-ferromagnetic.

The evolution of the peaks relative intensity for the Cr looks like the one for the Mn. Under magnetic field, the $S_z = -1$ is stabilized, becoming the lower energy state of the doublet $S_z = \pm 1$. For a high enough magnetic field, we can only consider the recombination toward $S_z = -1$. The high energy peak corresponds then to the $|S_z = -1, X_z = -1\rangle \rightarrow |S_z = -1\rangle$ on, emitting a $\sigma-$ polarized photon. The low energy one is associate with the $|S_z = -1, X_z = +1\rangle \rightarrow |S_z = -1\rangle$ transition, emitting a $\sigma+$ polarized photon. This is coherent with an anti-ferromagnetic coupling between the Cr and hole, contradicting the assumption made in Sec. **??** and confirming the energy structure presented in Fig. I.2.

I.2 Modelization of a Cr-doped QD

We calculated the magneto-optic behaviour of Cr-doped QDs by diagonalizing the complete Hamiltonian of the e-h-Cr in self-assembled dots. We use for this purpose a spin effective hamiltonian that can be separated as follows:

$$\mathcal{H}_{X-Cr} = \mathcal{H}_{Cr,\varepsilon} + \mathcal{H}_{cCr} + \mathcal{H}_{mag} + \mathcal{H}_{eh} + \mathcal{H}_{band} + \mathcal{H}_{scat} \tag{I.2}$$

where:

$\mathcal{H}_{Cr,\varepsilon}$ describes the fine structure of the Cr atom and its dependency on local strain, as presented in Eq. **??**. It is mainly drived by D_0, the magnetic anisotropy. E, the in-plane strain anisotropy, also appears in this Hamiltonian, but have to be kept small in order to model the found dots (see Fig. I.13 for the emission of a dot with a higher E).

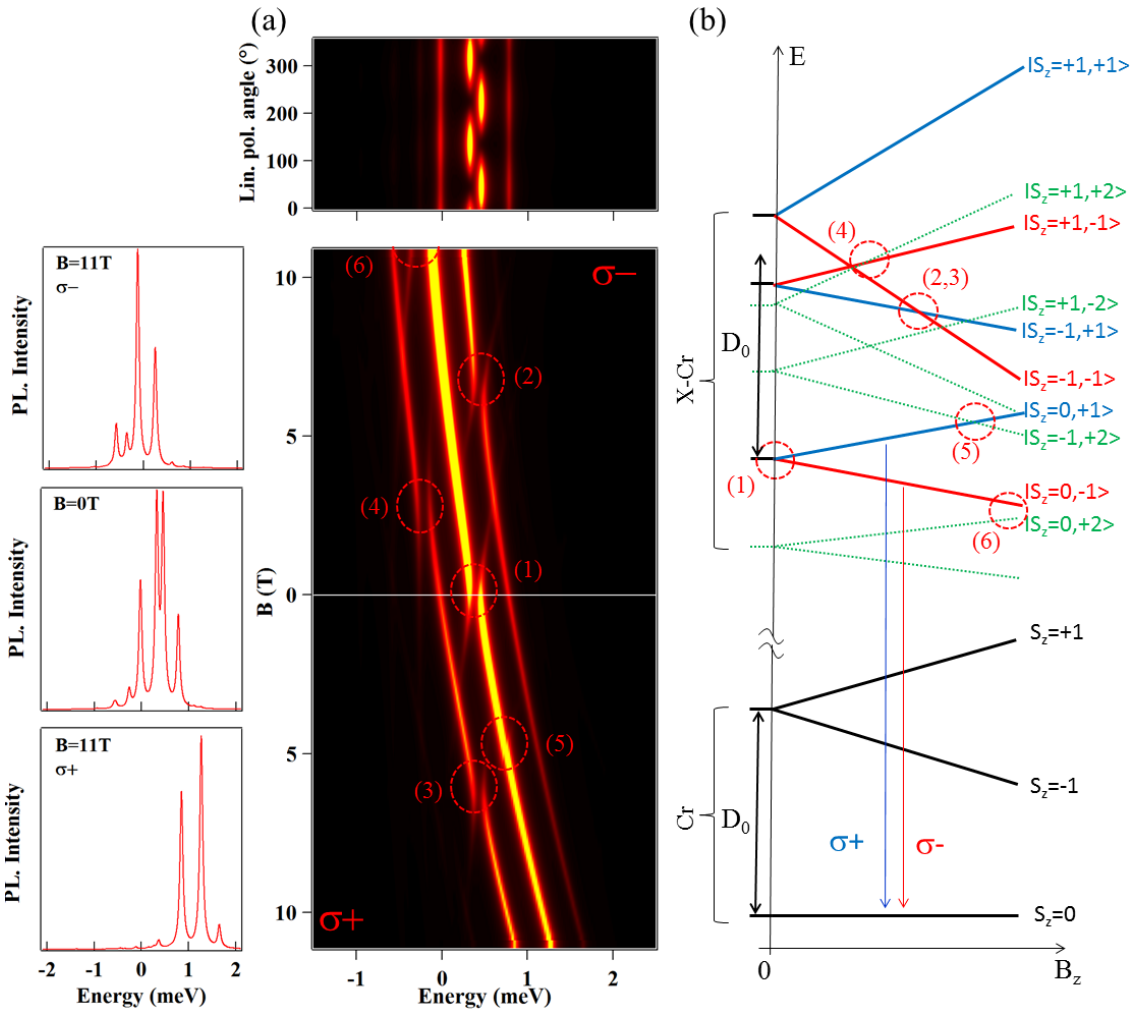

Figure I.12: (a) Top: Calculated linear polarization PL intensity map of X-Cr at zero field. The 0° polarization angle correspond to an emission polarized along the [100] axis. Bottom: Calculated X-Cr circularly polarized magnetic field dependency. Details of the model and parameters are listed in Tab. I.1. Corresponding anti-crossing are highlighted in same fashion as on Fig. I.8 and I.10. On the left, spectra calculated for $B_z = 0$ T and $B_z = 11$ T in both circular polarization are shown. (b) Schema of the magnetic field dependency of the energy levels of the low energy Cr spin states S_z=0 and S_z=±1, and corresponding bright ($|+1\rangle$ blue, $|-1\rangle$ red) and dark ($|\pm 2\rangle$ green) X-Cr energy levels.

$\mathcal{H}_{cCr}$ describes the coupling of the electron and hole with the Cr spin, depending on I_{eCr}, the exchange integral of the electron-Cr spins, and I_{hCr}, the exchange

integral of the hole-Cr spins, as described in Eq. ??.

$\mathcal{H}_{mag}$ describes the effect of an exterior magnetic field, coupled to both the Cr and carrier spins by the Zeeman terms, depending on the g-factor of each of them and the Bohr magneton μ_B, and including the diamagnetic shift of the electron-hole via the term γ.

$$\mathcal{H}_{mag} = g_{Cr}\mu_B \overrightarrow{B}.\overrightarrow{S} + g_e\mu_B \overrightarrow{B}.\overrightarrow{\sigma} + g_h\mu_B \overrightarrow{B}.\overrightarrow{J} + \gamma B^2 \tag{I.3}$$

$\mathcal{H}_{eh}$ describes the short range and long range electron-hole interaction, through the bright and dark exciton splitting δ_0, the bright exciton coupling δ_1, the dark exciton coupling δ_2 and the bright and dark exciton coupling δ_{11} and δ_{12}. All of these term are described in Eq ??.

$\mathcal{H}_{band}$ is the band Hamiltonian. It is written $\mathcal{H}_{band} = E_g + \mathcal{H}_{VBM}$, with E_g the CdTe gap energy and $\mathcal{H}_{VBM}$ is described in Eq. ??.

$\mathcal{H}_{scat}$ describes the perturbation of the wave function of the exciton in the initial state of the optical transition by the hole-Cr exchange interaction, controlled by the parameter η. It was found to be essential to explain the dynamic of X^+-Mn and is introduced here for generality purpose. This perturbation depends on the value of the exchange energy between the Cr spin S_z and the hole spin J_z and can be represented, using second order perturbation theory, by an effective spin Hamiltonian [14, 15, 17]

$$\mathcal{H}_{scat} = -\eta S_z^2 \tag{I.4}$$

with $\eta > 0$.

We considered the general case of QDs with a symmetry lower than C_{2v} (truncated ellipsoidal lens for instance [13]), and took into account the influence of this reduced symmetry on the valence band and on the e-h exchange interaction. The population of the X-Cr spin states split by the large magnetic anisotropy and the carriers-Cr exchange interaction is described by a spin effective temperature T_{eff}, applied on the X-Cr levels and the initial state of the hamiltonian. The results of the model obtained with T_{eff} =20K, $D_0 = 2.2$ meV and an electron-Cr (hole-Cr) exchange interaction $I_{eCr} = -50$ μeV ($I_{hCr} = 250$ μeV) are reported in Fig. I.12 (parameters not specific to Cr-doped QDs are listed in Tab. I.1). Such parameters do not aim to fit the data and are only reasonable order of magnitude to qualitatively reproduce the experimental results of the PL of X-Cr at zero field and its evolution in magnetic field. The splitting of the central line at zero field (anti-crossing (1)) and the anti-crossings under magnetic field (anti-crossings (2) and (3) around B_z=6T for the Cr spin states $S_z = |+1\rangle$ and anti-crossings (4) with the dark exciton around B_z=2T) are well reproduced by the model.

This model also predicts an anti-crossing around $B_z = 5$ T, noted (5), caused by an electron-Cr flip flop, which is not sawn on the experiments. Its position

Table I.1: Values of the parameters used in the model of Cr-doped CdTe/ZnTe quantum dot presented in Fig. I.12. The value of the parameters not listed in the table is 0. The chosen values are typical for CdTe/ZnTe quantum dots and can be compared with parameters extracted from Mn-doped quantum dots [8, 17]. These values are reasonable to reproduce the emission of the QDs presented in this thesis.

I_{eCr} μeV	I_{hCr} μeV	δ_0 meV	δ_1 μeV	δ_{12} μeV	δ_{11} μeV	$\frac{\lvert s\rvert}{\Delta_{lh}}$	$\frac{\lvert r\rvert}{\Delta_{lh}}$
-50	250	-1	250	150	50	0.05	0.05

arg(r)	D_0 meV	g_{Cr}	g_e	g_h	γ $\mu eV/T^2$	η μeV	T_{eff} K
$-\frac{\pi}{2}$	2.2	2	-1	0.4	1.5	25	20

is controlled by D_0 and its intensity by I_{eCr}. However, for this anti-crossing to appear for $B_z > 11$T, a $D_0 > 3$ meV is needed, causing the $S_z = \pm 1$ levels to be at high energy and thus giving a stronger emission intensity to the $S_z = 0$ state than the one sawn experimentally. Therefore, a low value of I_{eCr} was chosen instead. Finally, the remaining tail of an anti-crossing, labelled (6), also appears at high magnetic field in the $\sigma-$ polarization, as saw in Fig. I.10, due to the coupling a bright and a dark exciton coupled to the Cr state $S_z = 0$.

The magnetic anisotropy D_0 cannot be precisely extracted from the PL spectra. However, for $D_0 < 2$ meV, an anti-crossing due to a VBM induced hole-Cr flip-flop between the $|-1, +2\rangle$ and the $|0, -1\rangle$ would appear below B_z=11T on the central line in $\sigma-$ polarization. Moreover, as discussed earlier, a $D_0 > 3$ meV would produce a lower PL intensity for the states $S_z = \pm 1$. These consideration sets a D_0 in the range of 2 to 3 meV. However, even in this range, the intensity distribution of the PL cannot be perfectly reproduced: while the intensity ratio of the peaks is quite well predicted for high value of the magnetic field, the $S_z = 0$ state still present a stronger emission at $B_z = 0$T than the one observed in the experiments. This difference in intensity may be due to out of equilibrium phonons in the sample that help populating the $S_z = \pm 1$ states.

Our model reproduce qualitatively with enough satisfaction the data found experimentally and thus can be used to see the evolution of the emission varying different parameter. Especially, an interesting point is the influence of the anisotropy of strains on the emission. The results of the calculations are presented on Fig. I.13.

The linear polarization dependency of the PL shows a splitting of all the three peaks at 0T, strengthening for a higher anisotropy of strain. In-plane strain anisotropy lead to Valence Band Mixing via the Bir-Pikus hamiltonian, as pre-

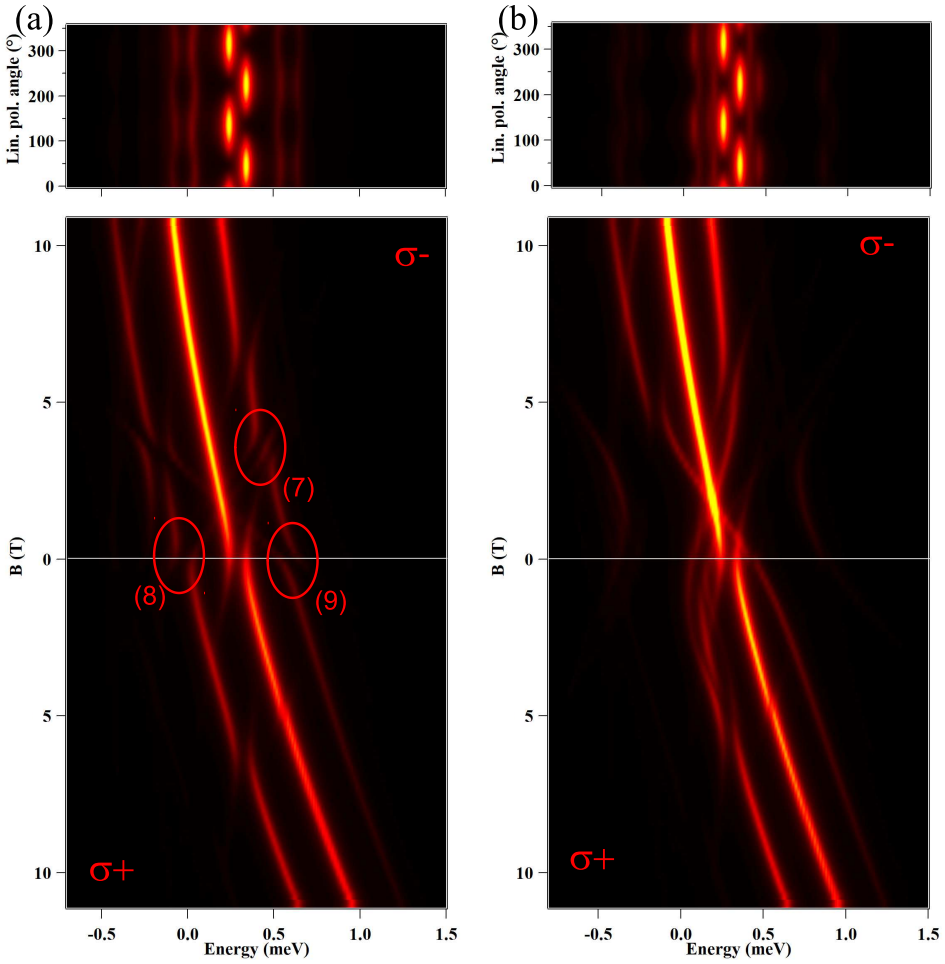

Figure I.13: Calculated X-Cr linear polarization intensity map at B = 0T (top) and circularly polarized magnetic dependency (bottom) for dot with an anisotropy of strains (a) $E = 25$ μeV and (b) $E = 100$ μeV.

sented in Sec. **??**. Bright excitons mixed this way presents a linearly polarized emission. However, bright excitons levels are split when coupled to Cr spin states $S_z = \pm 1$, acting as an effective magnetic field. A small anisotropy of strain cannot couple those, and thus they do not present linear polarization. Increasing the value of the anisotropy make it possible for these levels to be coupled, giving their emission a linear polarization dependency.

The anisotropy of strain also affects the anti-crossing appearing of the magnetic field dependency. The anti-crossings (1) through (6) remain but we decided not to highlight them for the sake of clarity. Three new anti-crossings appear when increasing the value of E. Anti-crossings (8) and (9), on the outside peaks at B =

0T, are caused E induced VBM discussed in the previous paragraph. Anti-crossing (7), on the high energy peak at roughly the same magnetic field value and direction as anti-crossing (4), appears when $|S_z = +1, X_z = -1\rangle$ and $|S_z = -1, X_z = -1\rangle$ are brought together by the magnetic field. They are coupled by the E term, coupling two levels separated by two units of spin, via an electron-hole flip flop.

For a higher value of E, the anti-crossings are stronger. They occur on a larger range of energy, and with a wider split for the anti-crossing (8) and (9). This leads to a superposition of the different anti-crossing, giving a complex magnetic dependency and the apparent reduction of the splitting at B = 0T.

Most of the dot we found presented a small anisotropy. The reason might be a selection bias. The splitting at zero magnetic field leads to a spectra with six different peaks. Moreover, we saw on Fig. I.13 (b) that the splitting at B = 0T can be reduced due to the width of the anti-crossings. The resolution of our monochromator might then not be precise enough to resolve the peaks, and only shows a broad emission. Such a dot would then not be selected for further studies, leading to a selection bias toward low anisotropy dots.

I.3 Charge fluctuation of a Cr ion in the vicinity of the QDs

Some dots were found presenting a linear polarization dependency all their peaks, for both X-Cr and X^2-Cr. One of them, QD5, is presented on Fig. I.14. Such a dependency is expected in dots with a strong in-plane anisotropy, as shown in Sec. I.2. While a thin and well resolve X^+-Cr is observed on all these dots, X-Cr is often not resolved, appearing as a broad emission. Such a result was also expected for dots with strong in-plan anisotropy.

However, studying the dot under magnetic field show no appearance of the expected anti-crossing for a QD with a high in-plane anisotropy. The dots present a single anti-crossing on all their peaks for B = 9T in $\sigma-$ polarization. It is due to the mixing between bright and dark exciton. Such an evolution under magnetic tend to characterise three non-magnetic QDs emitting at close energy. However, all the peaks were found to have the maximum intensity for the same position on the sample, and they share excited states on the PLE. It is highly improbable to find three dots close to each other, emitting almost at the same energy and sharing excited states at several position on the sample.

To further investigate those dots, we study the evolution of their emission under bias voltage. The application of an electric field was realized via a sample with a Schottky gate in the same fashion than the one in Fig. I.15(c). The resulting map is presented in Fig. I.15(a). The first visible feature is the strong electric

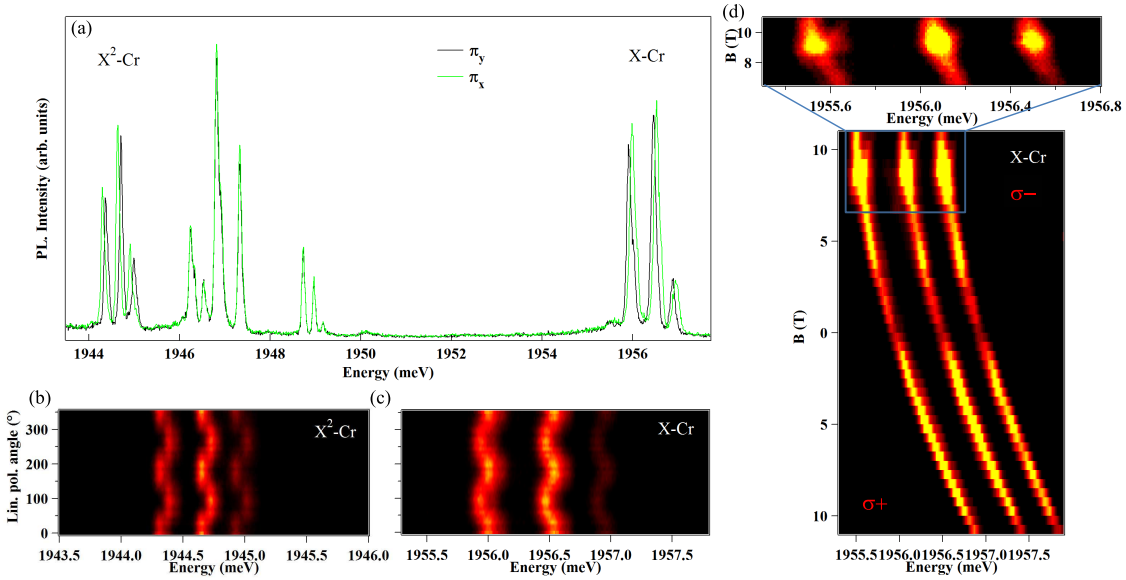

Figure I.14: (a) QD5 linearly polarized PL intensity at zero magnetic field. (b) and (c) Respectively QD5 X^2-Cr and X-Cr linear polarization PL dependence at zero magnetic field. (c) X-Cr magnetic field PL dependence of QD5. Zoom in presents anti-crossing appearing at B=9T.

field dependency of the emission energy, more marked for X-Cr than for the X^c-Cr systems. The emission energy variation of the X-Cr complex occurs in a 2.9 meV range.

There is another remarkable point on these maps, evidenced on the X^+-Cr complex on the Fig. I.15(b): the splitting between each peak is changing with the applied electric field. The splitting between the high and low energy peaks varies from 0 meV for an applied bias voltage of -8V (no splitting) to 0.7 meV for 8V applied. This disappearance of the splitting for a certain bias voltage indicates that phenomena inducing an emission at three different energy can be tuned using an external electric field.

Fig. I.16 shows that, using electric field, we can manipulate the splitting of any given charged state of the QD. For all positive bias voltage between 0V and 7V, X-Cr present a broad emission containing all six peaks in linear emission, as show on Fig. I.16(a). The emission then divide into three distinct peaks, starting to appear around -1V. This is evidenced on the the PL emission on Fig. I.16(d).

We propose that those dots particular PLs are caused by Cr in the ZnTe barrier close to the dot. Cr is incorporated in ZnTe as Cr^{2+}, but, as shown on Fig.I.17(a), the Cr^+ and Cr^{3+} states are in the gap and accessible [19], either by capturing

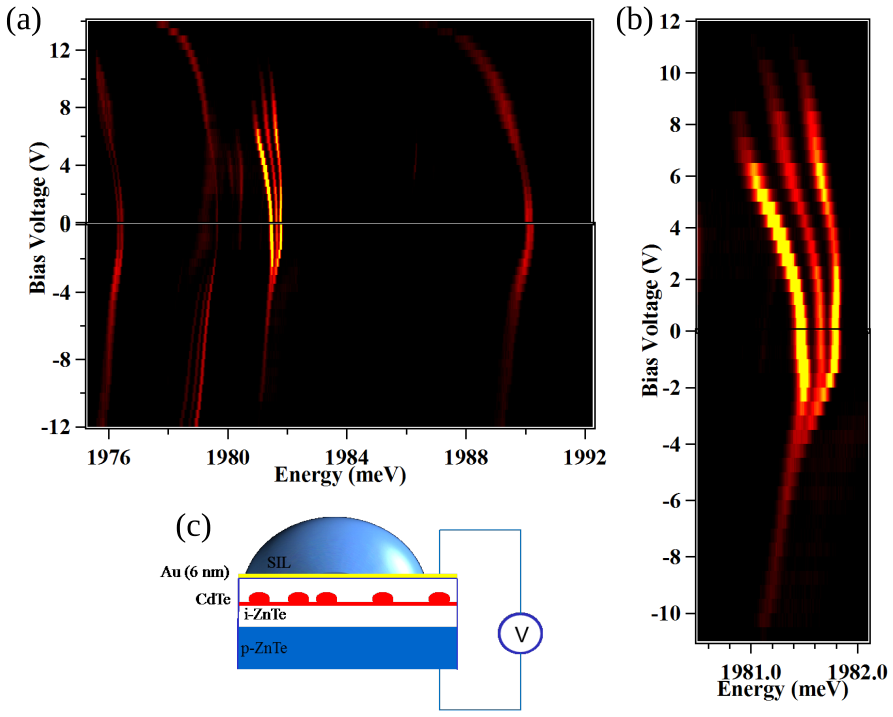

Figure I.15: (a) QD7 whole PL evolution under application of a bias voltage. (b) Zoom on X^c-Cr circular polarization PL intensity evolution under electric field. A strong stark shift is observed, as well as variation in the splitting. (c) Schema of a sample with a Schottky gate used to apply the bias voltage on the sample.

an electron (Cr^+) or a hole (Cr^{3+}). Considering such a charge close to the QD, it can be viewed as a punctual one, since the dot is far bigger than the atom. The effect on the wave functions, presented in Fig.I.17(b)-(d), differs depending on the electrical charge of the Cr atom. Cr^{2+} is the neutral state of Cr in ZnTe, sharing its outer shell electrons to bond with the atoms of the crystal. It is therefore the neutral position of the QD-Cr system. Capturing an electron, the Cr atom get a supplementary negative charge, and will thus attract more strongly the hole confined in the QD and repel the electron. The opposite happens when the Cr capture a hole.

The electron is well confined in CdTe/ZnTe quantum dots and will thus not be affected strongly by the presence of a punctual charge close to the QD. The hole, on the other hand, is only weakly confined in CdTe/ZnTe QDs. Its wavefunction will then be more strongly affected by the charge variations of the Chromium. This weak confinement also mean that the wavefunction goes slightly out of the dot, and thus the overlap with the Cr atom might exist for the hole, even if the

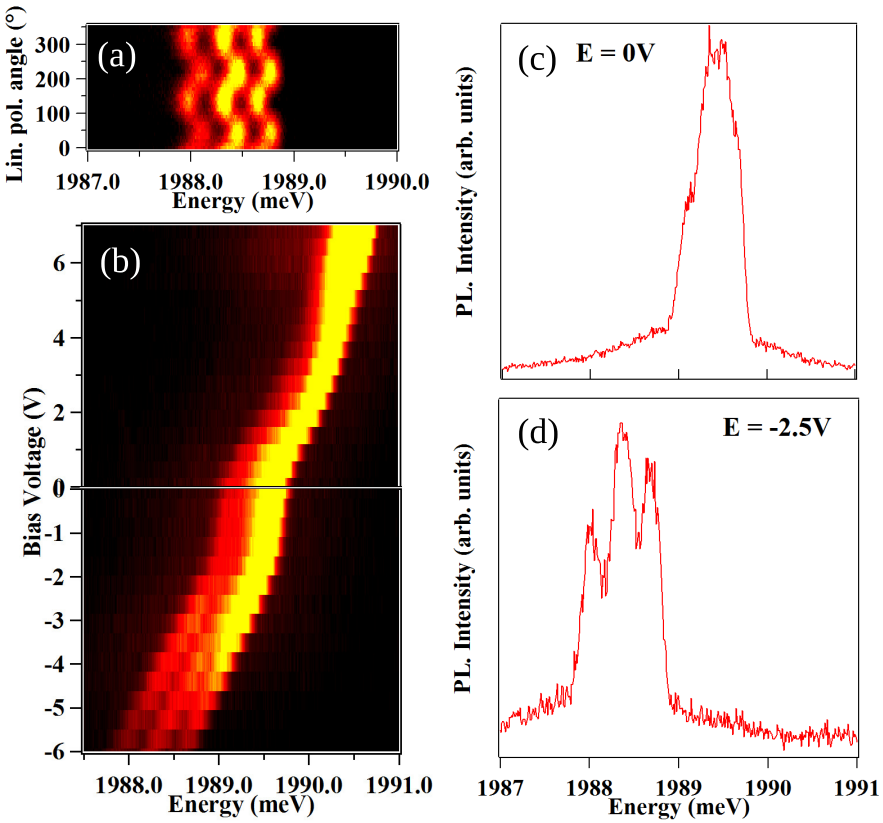

Figure I.16: All these measures were taken on QD8 X-Cr complex at low temperature. (a) PL intensity dependency in linear polarization. In order to have the best contrast, the map was taken at -2.5V bias voltage. (b) Circular PL intensity evolution in electric field. A splitting began to appear around -2V of applied bias voltage. (c)-(d) Circular PL for an applied bias voltage of, respectively, 0V and -2.5V.

atom is not in the QD. The slight overlap is enough to cause the splitting of the exciton emission PL via the exchange interaction, without the Cr being affected by the dot. When the atom get a positive charge, it will repel the hole, reducing the overlap until none remain, killing the splitting of the emission. The opposite happens when the Cr capture an electron, attracting the hole and improving the overlap. The overlap can also be affected by the application of a magnetic field through the Schottky gate, which will change the wavefunctions shape and the probability for the Cr atom to be in a given charge state.

This hypothesis is currently tested, along with the capacity for the Cr to diffuse outside the quantum dots layer.

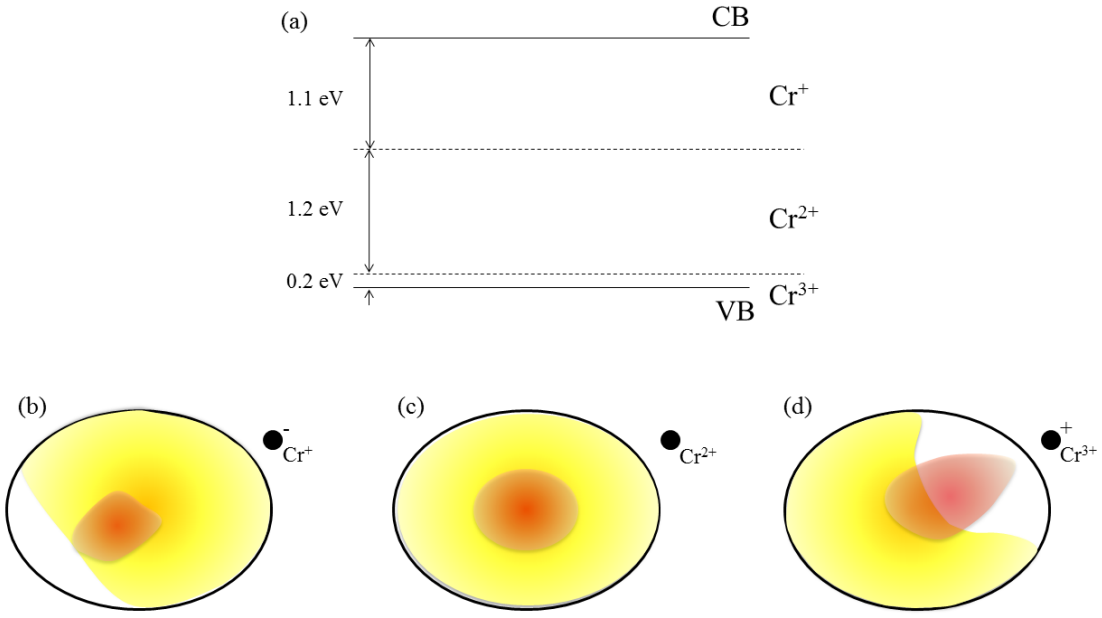

Figure I.17: (a) Cr accessible charged states in ZnTe. (b)-(d) Illustration of the effect of a punctual charge on the wavefunction of an electron (red) and a hole (yellow) in a quantum dots.

I.4 Conclusion

For the first time, a single Cr atom was embedded inside a II-VI quantum dot. We were then able to probe it optically. Such a system presents a characteristic three peak emission, along with the emission of a dark state on the low energy side. The action of the magnetic anisotropy, splitting the Cr spin states according to $D_0 S_z^2$, is strong enough to keep the $S_z = \pm 2$ level to be thermally populated, and thus they do not present luminescence. The QDs show a good spin conversation during the exciton lifetime inside the dot, thanks to the effective magnetic field created by the Cr spin. Magneto-optics confirm the chosen energy structure and gives us the possibility to deduce the magnitude of several of the quantum dot parameters. We used the model to simulate the emission of QD with different parameters, and proposed an explanation to the absence of high anisotropy QDs in the one we probed. Some dots seems to correspond to these high anisotropy QDs, but they show no sign of magnetic atom inside them under further investigation. We finished proposing a possible explanation for those dots, supposing the presence of Cr atoms in the ZnTe barrier.

Having successfully inserted a probed single Cr atom in CdTe/ZnTe quantum

dots, it is now important to study how this system evolve in time. An important step for further use of the system will be the possibility to prepare the Cr spin in a chosen state, and then control it. This is what we propose to study in the next chapter.

Bibliography

[1] J. T. Vallin and G. D. Watkins, "EPR of Cr^{2+} in II-VI lattices", Phys. Rev. B **9**, 2051–2072 (1974).

[2] M. Herbich, W. Mac, A. Twardowski, K. Ando, Y. Shapira, and M. Demianiuk, "Magnetization and exciton spectroscopy of the diluted magnetic semiconductor $\mathrm{cd}_{1-x}\mathrm{cr}_x\mathrm{s}$", Phys. Rev. B **58**, 1912–1921 (1998).

[3] P. Kacman, "Spin interactions in diluted magnetic semiconductors and magnetic semiconductor structures", Semicond. Sci. Technol. **16**, R25 (2001).

[4] W. Mac, A. Twardowski, and M. Demianiuk, "S,p-d exchange interaction in Cr-based diluted magnetic semiconductors", Phys. Rev. B **54**, 5528–5535 (1996).

[5] W. Mac, A. Twardowski, and M. Demianiuk, "s,p-d exchange interaction in Cr-based diluted magnetic semiconductors", Phys. Rev. B **54**, 5528–5535 (1996).

[6] M. Herbich, W. Mac, A. Twardowski, K. Ando, Y. Shapira, and M. Demianiuk, "Magnetization and exciton spectroscopy of the diluted magnetic semiconductor $Cd_{1-x}Cr_xS$", Phys. Rev. B **58**, 1912–1921 (1998).

[7] T. Takagahara, "Theory of exciton doublet structures and polarization relaxation in single quantum dots", Phys. Rev. B **62**, 16840–16855 (2000).

[8] M. Bayer, G. Ortner, O. Stern, A. Kuther, A. A. Gorbunov, A. Forchel, P. Hawrylak, S. Fafard, K. Hinzer, T. L. Reinecke, S. N. Walck, J. P. Reithmaier, F. Klopf, and F. Schäfer, "Fine structure of neutral and charged excitons in self-assembled In(Ga)As/(Al)GaAs quantum dots", Phys. Rev. B **65**, 195315 (2002).

[9] J. McFarlane, P. A. Dalgarno, B. D. Gerardot, R. H. Hadfield, R. J. Warburton, K. Karrai, A. Badolato, and P. M. Petroff, "Gigahertz bandwidth electrical control over a dark exciton-based memory bit in a single quantum dot", Applied Physics Letters **94**, 093113 (2009).

[10] D. Gammon, E. S. Snow, B. V. Shanabrook, D. S. Katzer, and D. Park, "Fine structure splitting in the optical spectra of single GaAs quantum dots", Phys. Rev. Lett. **76**, 3005–3008 (1996).

[11]L. Besombes and H. Boukari, "Resonant optical pumping of a Mn spin in a strain-free quantum dot", Phys. Rev. B **89**, 085315 (2014).

[12]Y. Léger, L. Besombes, L. Maingault, D. Ferrand, and H. Mariette, "Geometrical effects on the optical properties of quantum dots doped with a single magnetic atom", Phys. Rev. Lett. **95**, 047403 (2005).

[13]M. Zieli ński, Y. Don, and D. Gershoni, "Atomistic theory of dark excitons in self-assembled quantum dots of reduced symmetry", Phys. Rev. B **91**, 085403 (2015).

[14]L. Besombes, Y. Leger, L. Maingault, D. Ferrand, H. Mariette, and J. Cibert, "Carrier-induced spin splitting of an individual magnetic atom embedded in a quantum dot", Phys. Rev. B **71**, 161307 (2005).

[15]A. H. Trojnar, M. Korkusinski, U. C. Mendes, M. Goryca, M. Koperski, T. Smolenski, P. Kossacki, P. Wojnar, and P. Hawrylak, "Fine structure of a biexciton in a single quantum dot with a magnetic impurity", Phys. Rev. B **87**, 205311 (2013).

[16]Y. Léger, "Détection de spins individuels dans les boîtes quantiques magnétiques", Theses (Université Joseph-Fourier - Grenoble I, Sept. 2007).

[17]B. Varghese, H. Boukari, and L. Besombes, "Dynamics of a Mn spin coupled to a single hole confined in a quantum dot", Phys. Rev. B **90**, 115307 (2014).

[18]H. Kamada and T. Kutsuwa, "Broadening of single quantum dot exciton luminescence spectra due to interaction with randomly fluctuating environmental charges", Phys. Rev. B **78**, 155324 (2008).

[19]J. Dziesiaty, P. Peka, M. U. Lehr, A. Klimakow, S. Müller, and H.-J. Schulz, "The chromium impurity in znte: changes of the charge state detected by optical and EPR spectroscopy", ZPCH **201**, 63 (1997).

[20]A. Barfuss, J. Teissier, E. Neu, A. Nunnenkamp, and P. Maletinsky, "Strong mechanical driving of a single electron spin", Nat Phys **11**, 820 (2015).

[21]A. Lafuente-Sampietro, H. Boukari, and L. Besombes, "Strain-induced coherent dynamics of coupled carriers and Mn spins in a quantum dot", Phys. Rev. B **92**, 081305 (2015).